Genetics: Early Online, published on April 8, 2015 as 10.1534/genetics.115.176917

Multiplex conditional mutagenesis using transgenic expression of cas9 and sgRNAs

Linlin Yin*, Lisette A Maddison*, Mingyu Li*, Nergis Kara[§], Matthew C LaFave[†], Gaurav K Varshney[†], Shawn M Burgess[†], James G Patton[§] and Wenbiao Chen*

*Department of Molecular Physiology & Biophysics, Vanderbilt University School of Medicine, Nashville, TN 37232, USA

[§] Department of Biological Science, Vanderbilt University, Nashville, TN 37240, USA

[†] Translational and Functional Genomics Branch, National Human Genome Research Institute, National Institutes of Health, Bethesda, MD 20892, USA

Copyright 2015.

Running Title: Multiplex conditional mutagenesis

Key words: CRISPR/Cas9, conditional mutagenesis, glucose homeostasis, retinal regeneration, zebrafish

Corresponding author:

Wenbiao Chen

702 Light Hall

2215 Garland Avenue

Nashville, TN 37232

Tel:1-615-936-8126

Fax: 1-615-322-7236

Email: wenbiao.chen@vanderbilt.edu

ABSTRACT

Determining the mechanism of gene function is greatly enhanced using conditional mutagenesis. However, generating engineered conditional alleles is inefficient and has only been widely used in mice. Importantly, multiplex conditional mutagenesis requires extensive breeding. Here we demonstrate a system for one-generation multiplex conditional mutagenesis in zebrafish (Danio rerio) using transgenic expression of both *cas9* and multiple sgRNAs. We describe five distinct zebrafish U6 promoters for sgRNA expression and demonstrate efficient multiplex biallelic inactivation of *tyrosinase*, *insulin receptor a* and *b,* resulting in defects in pigmentation and glucose homeostasis. Furthermore, we demonstrate temporal and tissue-specific mutagenesis using transgenic expression of Cas9. Heat-shock inducible expression of *cas9* allows temporal control of *tyr* mutagenesis. Liver-specific expression of *cas9* disrupts *insulin receptor a* and *b,* causing fasting hypoglycaemia and postprandial hyperglycemia. We also show that delivery of sgRNAs targeting *ascl1a* into the eye leads to impaired damage-induced photoreceptor regeneration. Our findings suggest that CRISPR/Cas9-based conditional mutagenesis in zebrafish is not only feasible but rapid and straightforward.

INTRODUCTION

Conditional gene inactivation is necessary for determining physiological functions of genes whose conventional mutation causes embryonic lethality or multi-organ defects. It has been widely used in mice because of the availability of embryonic stem cells (ES) cells and large collections of both ES cell lines and animals that carry conditional alleles. The conditional alleles usually contain strategically placed Cre or Flp target sites in introns that permit deletion of the intervening exon(s) (GU *et al.* 1994). Some conditional alleles harbor a Cre and/or Flp invertible gene-trap in an intron that allow on/off switch of transcription (SCHNUTGEN *et al.* 2005) (NI *et al.* 2012). The function or expression of these alleles is "switched" off in the presence of Cre or Flp activity. In Drosophila, conditional gene inactivation can be achieved using RNAi, and genome-wide libraries of RNAi transgenes are available (DIETZL *et al.* 2007; NI *et al.* 2008). For the increasingly popular zebrafish model, however, only limited conditional alleles generated from invertible gene-trapping are available (NI *et al.* 2012). The lack of ES cells and the inefficiency of RNAi in zebrafish necessitate new approaches for targeted conditional gene inactivation.

CRISPR/Cas9 mutagenesis has been applied to many model systems from cultured cells to whole organisms (DOUDNA and CHARPENTIER 2014; HSU *et al.* 2014). The system only requires a two-component RNA-Protein complex (RNP): a single guide RNA (sgRNA) that identifies the target through base-pairing, and the Cas9 endonuclease that generates double strand breaks at the target site upon sgRNA-target base paring. CRISPR/Cas9 mutagenesis has been widely used in zebrafish (CHANG *et al.* 2013; HWANG *et al.* 2013; JAO *et al.* 2013), where mutagenesis is usually achieved by injecting zygotes with in vitro synthesized Cas9 mRNA and sgRNA, or sgRNA-Cas9 RNP (GAGNON *et al.* 2014; SUNG *et al.* 2014). This generates

germline mutations as well as mosaic somatic mutations in all tissues. The mutagenesis in somatic cells is sufficient to cause extensive biallelic mutations and phenotypes in injected animals (JAO *et al.* 2013). Given the effectiveness of this system, we set out to determine whether transgenic expression of *cas9* and sgRNA can generate biallelic mutations and whether the CRISPR system can be adopted for targeted conditional mutagenesis. Here we report tissue-specific and inducible multiplex mutagenesis in zebrafish using transgenic lines expressing Cas9 and sgRNA.

MATERIAL AND METHODS

Zebrafish strains and maintenance

Zebrafish were raised in an Aquatic-Habitats system on a 14-/10-h light/dark cycle. Embryos were obtained from natural crossing and raised at 28.5ºC in an incubator with lights on a 14-/10-hour light/dark cycle. Animals were staged by days post-fertilization (dpf) or in months of age. At 5 dpf, fish were placed on the normal rearing diet and maintained as per standard protocols until appropriate age. All procedures have been approved by the Vanderbilt University IACUC Committee.

Plasmid Construction

Transgenes were generated using the Tol2-based Multisite Gateway system (KWAN *et al.* 2007). For Cas9-expression transgenes, the codon optimized *nls-cas9-nls* (JAO *et al.* 2013) was cloned into pME-MCS to generate pME-cas9. The broadly expressed promoters *actb2* and *ubi*, and the HotCre promoter were cloned into p5E-MCS. pDestTol2LR was made by inserting a 1.95kb BglII fragment containing cryaa:tagRFP into the BglII site of pDestTol2pA2. To generate the sgRNA expression cassette, the U6a promoter was obtained by using U6aF1

and U6aR1 and inserted into the HindIII/PstI sites of pT7-gRNA to replace the T7 promoter (Jao et al., 2013). The sgRNA core was then replaced with sgRNA^{EF} to facilitate U6 guided transcription (CHEN *et al.* 2013). A transcription stop for U6, TTTTTT, was then added at the 3' end of sgRNA core by PCR. The cassette was then inserted into a miniTol2 vector to generate pT2-U6a:sgRNA (URASAKI *et al.* 2006). Other U6 promoters (U6b, U6c, U6d and U6e) were amplified using primers listed in Supplemental Table 1 and inserted into the ApaI/XhoI sites in pT2-U6a-sgRNA to replace U6a.The protospacer for *tyr* was inserted into pT2-U6a:sgRNA by annealing tyr-F and tyr-R and ligated in the presence of BsmBI as described (Jao et al., 2013). Protospacers for EGFP, *insra* and *insrb* were ligated in the presence of BsmBI after annealing the primer pairs listed in Supplemental Table 1. To allow orderly assembly using Golden Gate ligation, BsaI sites were added via PCR on both ends of the *U6:sgRNA* cassettes using primers listed in Supplemental Table 1. PCR products were inserted into the ApaI/XbaI sites of pLR-NN from the Golden Gate TALEN kit obtained from Addgene (CERMAK *et al.* 2011). The destination vector for these *U6x:sgRNA* cassettes were made first by eliminating the BsaI site in pDestTol2CG2 (KWAN *et al.* 2007), followed by replacing the cmcl2:EGFP (AatII/KpnI) with a *cryaa:mCerulean* (SacII/KpnI) from phsp70l-loxP-mCherry-STOP-loxP-H2B-GFP_cryaa-cerulean to generate pDestTol2LC (HESSELSON *et al.* 2009). Two BsaI site-containing adaptors with appropriate overhang were sequentially inserted into the NsiI/XhoI and KpnI sites of pDestTol2LC, resulting in the pGGDestTol2LC series. All relevant plasmids have been deposited to Addgene for distribution (Supplemental Methods).

Transgenesis

To generate transgenic fish, the mixture of Tol2 RNA (25pg) and plasmid (20pg) was injected into the cell of one-cell stage embryos. Then injected embryos were cultured with egg water in 28°C incubator for 5 days. After pre-screening for fluorescence, the positive larvae were raised in Aquatic Habitats systems on a 14-/10- h light/dark cycle until adult stage.

Semi-quantitative RT-PCR analysis

Total RNA of transgenic larvae was isolated using TRIzol (Invitrogen). After treated with DNase (New England Biolabs) for 30 min, reverse transcription was performed using M-MLV reverse transcriptase (Promega), RNase inhibitor (New England Biolabs), 2μg total RNA, oligo dT (for *actin* and *cas9*) or sgRNA specific oligo (5'- TTGCACCGACTCGGTG-3'). To detect the gene expression level, PCR reactions were prepared according to GoTaq® Flexi DNA Polymerase instructions (Promega). β-*actin*, *cas9* and sgRNA were amplified from cDNA by PCR with the primers listed in Supplemental Table 1. The PCR conditions were 95°C for 5min; 22 (β-*actin),* 28 (*sgRNA*), or 30 (*cas9*) cycles of 30 s at 95°C, 30s at 60°C and 30 s at 72°C; followed by 72°C for 5min.

Heteroduplex mobility assay

DNA was isolated with 50mM NaOH and then neutralized with 1M Tris.HCl. After amplification with GoTaq® Flexi DNA Polymerase (Promega) using genotyping primers, heteroduplex DNA was formed using the following parameters: 95°C for 5min; 95-85°C at -2°C/s; 85-25°C at -0.1°C/s; hold at 16°C. Samples were separated on a non-denaturing 10% polyacrylamide gel [10% acrylamide (29:1), 1× TBE, 0.05% ammonium persulfate, 0.05% TEMED] and run in 1× TBE buffer. After running, the gel was stained with ethidium bromide

(0.5 μg/ml) and imaged by Gel Doc EZ System (Bio-Rad). The percentage of signal from the unmutated amplicon in each lane was quantified by Image Lab Software (Bio-Rad) and normalized to that of wild-type lanes. The mutation rate is the complement of the normalized percentage.

Assessing mutagenesis rate using quantitative PCR analysis

To determine the mutagenesis rate using qPCR (Yu *et al.* 2014), a fraction of the *tyr* PCR product used for HMA assay was diluted 50,000x. The diluted products were subjected to two sets of qPCR analyses: one set with primers >40 bp away from the Cas9 cut site to amplify both wild-type and mutant alleles, and the other with one primer encompassing the Cas9 cut site which should only amplify the wild type allele. qPCR was performed by Bio-Rad CFX96 Real-Time system with SYBR Green Supermix (Bio-Rad) using the following program: 40 cycles of 10 s at 95°C and 30 s at 60°C after initial denaturing for 3 min at 95°C. The primer pairs were listed in Supplemental Table 1.

Feeding and Glucose Measurement

For 5% egg yolk feeding, chicken egg yolk was separated and then diluted to 5% with 0.3× Danieau buffer. Egg yolk solution were shaken every 30min to maintain suspension. Before glucose measurement, fish were rinsed with 0.3× Danieau buffer three times. Glucose level of individual larvae was measured using Amplex® Red Glucose/Glucose Oxidase Assay Kit (Invitrogen). For blood glucose in adult animals, fish were either fasted overnight or fed as normal and blood collected 30 minutes after the meal. Blood was collected from the dorsal aorta along the trunk of the fish as indicated in Zang et al. (Zang *et al.* 2013). Blood glucose was determined as described (Li *et al.* 2014).

Imaging

Larvae were anesthetized with 0.01% MESAB (MS-222 or Tricaine) in 0.3× Danieau and then mounted in 3% methylcellulose. Images were taken by Zeiss Axio Imager Z1 microscope equipped with a Zeiss AxioCam MRm digital camera.

sgRNA injection and Immunohistochemistry

sgRNA was synthesized by annealing a T7 promoter-containing gene-specific primer ascl1a^{sgRNA}1 and ascl1a^{sgRNA}2 with sgRNA scaffold primers. The anneal oligos were filled-in with T4 DNA polymerase in the presence of 50µM dNTP (New England Biolabs). The resultant dsDNA was used as template for T7 RNA polymerase using MaxiScript T7 kit (Invitrogen). The sgRNA(*ascl1a*)s were combined and the mixture was injected into one eye (50ng/eye) of adult *Tg(actb2:cas9; LR)* fish followed by electroporation prior to light lesioning as described (THUMMEL *et al.* 2008). Collection, fixation, embedding, sectioning and immunohistochemistry (IHC) of injected *Tg(actb2:cas9; LR)* eyes were performed as described (RAJARAM *et al.* 2014).

High-throughput sequencing

Genomic DNA from individual larvae was extracted using 50mM NaOH and then neutralized with 1M Tris.HCl. The targeted regions of *tyr*, *insra* and *insrb* were amplified using gene specific primer pairs with the forward primer containing M13 forward promoter sequence (Supplemental Table 1) and a third M13 forward promoter-based barcode primer. After amplification, PCR products were purified using a QIAquick PCR purification kit (Qiagen) and products pooled together. The sequencing library was made from 100ng PCR products using the Ovation Ultraflow Library system (NuGen Inc.), quantified by qPCR (KAPA BioSystems). Around twenty-five million 300-base read pairs were generated and the sequence data was

processed using RTA version 1.18.54 and CASAVA version 1.8.2. Only about one million reads have a barcode.

Sequencing analysis

The detection of variants within 20 bp of the predicted cut site (or between two predicted cut sites) was performed by version 1.1 of the ampliconDIVider software (https://github.com/mlafave/ampliconDIVider). Briefly, ampliconDIVider first trims off non-genomic DNA, and then uses novoalign to align the reads to amplicons of interest (chr15:42572556-42572836 for *tyr*, chr2:37298862-37298953 for *insra*, and chr22:11114676-11114957 for *insrb*) in version Zv9 of the zebrafish genome assembly. It loops through each sample and uses the programs bam2mpg and mpg2vcf to identify if there were any deletions or insertions in the sample (http://research.nhgri.nih.gov/software/bam2mpg/)(TEER *et al.* 2010). As ampliconDIVider was designed for germline samples, the intermediate BAM files were analysed manually for variants detection in somatic samples. The scripts can be found at https://github.com/mlafave/ampliconDIVider/blob/master/sh/yin_targeted_crispr_frameshift_count.sh. The number of wild type reads and reads with mutations in the aforementioned distance from the predicted cut site were counted for mutation rate calculation.

RESULTS

Transgenic expression of Cas9 and *sgRNA*(*tyr)* results in hypopigmentation

We set out to test whether transgenic expression of Cas9 and sgRNA targeting a gene of interest (*goi*) can cause biallelic mutagenesis (Fig 1A). As a pilot experiment, we tested whether ubiquitous expression of Cas9 would cause a pigmentation defect in the presence

of *sgRNA* targeting *tyrosinase*. Tyrosinase is essential for vertebrate pigmentation and its loss of function leads to an easily recognizable albino phenotype (SEARLE 1990). Using Gateway assembly and Tol2 transgenesis (URASAKI *et al.* 2006; KWAN *et al.* 2007), we generated multiple transgenic lines expressing nls-Cas9-nls (hence referred to as Cas9 or *cas9*) (JAO *et al.* 2013). The zebrafish *ubiquitin* or *beta2-actin* promoter was used to drive *cas9* expression because of their high and ubiquitous activity (MOSIMANN *et al.* 2011; HIGASHIJIMA *et al.* 1997; BOONANUNTANASARN *et al.* 2008). Each transgene also carried a cassette for cardiac specific EGFP (CG), or lens specific tagRFP (LR), respectively, for genotyping. We compared the levels of *cas9* expression in seven lines of *Tg(ubi:cas9; CG)* using semi-quantitative RT-PCR and raised F1s from two lines with high expression for additional experiments. We used a zebrafish U6 promoter (U6a) to drive transcription of an sgRNA targeting *tyrosinase* (referred as *sgRNA(tyr)* henceforward) (JAO *et al.* 2013) and marked it with lens specific mCerulean (LC) for genotyping. Ten germline-transmitting *Tg(U6a:sgRNA(tyr); LC)* founders were identified. They were crossed to F1s from a *Tg(ubi:cas9; CG)* line to identify suitable *Tg(U6a:*sgRNA(*tyr); LC)* lines. Double transgenic larvae from *Tg(ubi:cas9; CG)* x *Tg(U6a:* sgRNA(*tyr); LC)* had various degrees of pigmentation in the retinal pigment epithelium (RPE) at 2 day-postfertilization (dpf) (Fig 1B), while single transgenic progeny, *Tg(U6a:*sgRNA(*tyr); LC)* or *Tg(ubi:cas9; CG)* did not show any abnormal pigmentation phenotypes (Fig 1C and 1D). The line with the most severe phenotype was propagated. The *Tg(U6a:*sgRNA(*tyr); LC)* F1s were used to identify the best *Tg(actb2:cas9; LR)* line from 12 founders for additional experiments (Fig 1E). Again, single transgenic progeny, *Tg(U6a:*sgRNA(*tyr); LC)* , or *Tg(actb2:cas9; LR)* did not show any abnormal pigmentation phenotypes (Fig 1F and 1G). To verify mutagenesis, we estimated the degree of mutagenesis in the double carrier progeny of the selected lines using a heteroduplex

mobility assay (HMA) where the PCR product encompassing the target region was separated on a 10% non-denaturing polyacrylamide gel followed by densitometry (Fig 1H). Heteroduplexes have a slower mobility due to an open single-strand configuration surrounding the mismatched region (OTA *et al.* 2013). HMA indicated that 61-90% of the *tyr* loci were mutated in double transgenic larvae at 5-day-post fertilization (dpf). To validate the HMA approach, we determined the mutagenesis rate in the same fish using a quantitative PCR approach that uses a primer encompassing the Cas9 cleavage site to measure a decreased presence of the wild-type allele (YU *et al.* 2014). As shown in Figure 1I, there was an excellent agreement between the two assays. We used HMA to determine the mutagenesis efficiency henceforth. Thus, transgenically expressed CRISPR components are sufficient to cause biallelic gene inactivation in zebrafish.

Development of a system for multiplex CRISPR/Cas9 mutagenesis in transgenic fish

We next tested whether multiplex mutagenesis is possible using the same transgenic approach. Multiplex CRISPR/Cas9 mutagenesis is desirable for several reasons. First, it allows the expression of multiple sgRNAs to target the same gene, likely increasing mutagenesis. Second, it may facilitate gene-gene interaction studies. Third, by targeting related genes, it can overcome functional redundancy, a concern particularly applicable in zebrafish because of the common presence of duplicated genes. To minimize potential instability of tandem sgRNA-expressing transgenes, we sought to use distinct *U6* promoters (Fig 2A). In addition to U6a cluster on chromosome 21, three other U6 clusters have been previously described on chromosome 3 (*U6e*), 9 (*U6b*) and 11 (*U6c)*, in zebrafish (HALBIG *et al.* 2008; CLARKE *et al.* 2012). We identified a fifth *U6* cluster on chromosome 6 (*U6d*). The

promoters for these U6 genes are divergent, with sequence identity less than 68% in the 400-bp upstream region (Fig 2A). We obtained *U6b* to *U6e* promoters using PCR.

We developed a Golden Gate ligation strategy to streamline the assembly of multiple sgRNA expression cassettes. This allowed ordered assembly of up to five *U6x:sgRNA* cassettes into a Tol2-based pGGDestTol2LC (Fig 2D, Supplemental Methods). To compare the activity of the five *U6* promoters, we used them to direct the expression of *sgRNA* targeting five genes, *atp2a2a*, *atp2a2b*, *nf1a*, *nf1b*, and *dmd*, whose somatic mosiacism is associated with human diseases (BIESECKER and SPINNER 2013). We assembled the expression cassettes in pGGDestTol2LC. RT-PCR analysis of the each sgRNA indicated that U6e promoter is less active while the other four promoters have similar activity (Fig 2B). To confirm that U6e promoter activity is lower, we used U6a, U6b and U6e to direct expression of sgRNA against *tyr*, *csf1r* (PARICHY *et al.* 2000) and *mpv17*(KRAUSS *et al.* 2013), key genes responsible for the three pigment cell types in zebrafish. The three cassettes were placed in pGGDestTol2LC and the construct was injected to generate stable lines. RT-PCR analysis of the F1 also indicated that U6e is less active (Fig 2C). We therefore chose the *U6a-d* promoters for multiplex sgRNA expression. Since *U6a:sgRNA(tyr)* cassette could serve as an mutagenesis indicator, it may be included in the multiplex sgRNA expression construct, leaving space for four additional cassettes (Fig 2D).

Inactivation of insra and insrb impairs glucose metabolism

As a test case for multiplex CRISPR mutagenesis, we chose *insulin receptor* genes as targets. Unlike mouse, zebrafish has two *insulin receptor* genes, *insra* and *insrb* (TOYOSHIMA *et al.* 2008). We targeted a region with 2 adjacent high quality sgRNAs in the 5' portion of each gene. The expression cassettes for the four sgRNAs, along with that of *sgRNA(tyr)*, were

placed in pGGDestTol2LC (Fig 3A). The targets for *insra* sgRNAs were located in exon 3, and those for *insrb* sgRNAs, exon 2 (Fig 3B). The construct was introduced into zebrafish and fourteen germline transmitting founders were identified. For simplicity, we refer to these lines as *Tg(U6x:sgRNA(insra/b); LC)*. To make sure that the four U6 promoters had equivalent activity, we compared the levels of transcripts from each U6 promoter. Semi-quantitative RT-PCR indicated they had similar activity in individual F1s (Fig 3C).

To determine whether multiplex mutagenesis occurs efficiently, we crossed the fourteen germline transmitting *Tg(U6x:sgRNA(insra/b); LC)* founders to *Tg(actb2:cas9; LR).* All *Tg(U6x:sgRNA(insra/b); LC); Tg(actb2:cas9; LR)* double carriers, as identified by having both CFP and RFP signal in the lens, had visible pigmentation phenotype in the RPE, although the severity of the phenotype varied. HMA analysis of 5 dpf double carriers from the line with the most severe pigmentation phenotypes confirmed efficient mutagenesis at the *tyr*, *insra* and *insrb* loci (Fig 3D). Importantly, the mutation rates at *tyr* in hypopigmented *Tg(U6x:sgRNA(insra/b); LC); Tg(actb2:cas9; LR)* larvae were comparable to those in *Tg(U6a:sgRNA(tyr); LC); Tg(actb2:cas9; LR)* (Fig 1H, 3D), implying sufficient Cas9 activity even when multiple sgRNAs were expressed. The HMA indicated that about 70-90% of *insra* and *insrb* were mutated in larvae exhibiting hypopigmentation (Fig 3D).

We selected 2 lines for high throughput sequencing analysis to determine the mutation spectrum and to more accurately measure the mutation rates. One line had the most severe pigmentation phenotypes while the other had modest phenotypes but high germline transmission rate. Within these lines, the severity of the pigmentation phenotypes still varied somewhat within the same clutch. We analysed the amplicons encompassing the three targets from twelve double carriers from the line with weak pigmentation phenotypes

and five double carriers from the line with severe pigmentation phenotypes (Supplemental Tables 2-5). The mutation rate at *tyr* determined by sequencing correlated with the severity of the pigmentation phenotypes. The group with severe pigmentation phenotypes had a mean mutation rate of 57.5%, while the group with modest pigmentation phenotypes had a mean mutation rate of 41.7%. In addition, the mutation rate is more variable in the group with modest phenotype, possibly due to subpopulations of independent germline insertions (Supplemental Table 2). Nevertheless, the degree of mutagenesis in the seventeen double carriers was positively correlated with each other in the same fish (*insra vs. tyr*, r^2=0.72; *insrb vs. tyr*, r^2=0.71) (Fig 3E), confirming our expectation that the severity of pigmentation phenotype may be a good predictor of the mutagenesis efficiency at the other targets. Sequence analysis in *insra* and *insrb* provided evidence for the benefit of using 2 sgRNAs. In addition to increase the mutagenesis efficiency, two sgRNAs also resulted in deletion of the intervening sequence, leading to a prominent product in the PCR reaction that constituted close to 30% of the indels in *insra* and 15% of the indels in *insrb* (Fig 3F, Supplemental Table 3 and 4). These deletions would be expected to result in complete loss of function. Sequencing analysis also revealed extremely high mosaicism which was expected from transgenic expression of CRISPR/Cas9 since mutagenesis should occur after maternal-zygotic transition at 1000-cell stage (KANE and KIMMEL 1993). More than 3511 *insra* alleles were identified in an individual from which about 75k reads were obtained. Despite the diversity, however, a set of highly frequent alleles was found in all the individuals. For example, the top three alleles of each locus were the same among the fish in the group with severe phenotypes and they constituted about 40% of all the reads in each individual (Fig 3F). The same three alleles were also identically ranked in the other group (Supplemental Table 3-5). As expected, one of the top alleles for *insra* and *insrb* was from precise deletion between

the two DSBs. The prevalence of other common deletions suggested that the NHEJ repair is not random. Inspection of the DSB-flanking sequences suggested that the most frequent alleles may result from microhomology-mediated repair (Supplemental Figure 1), supporting previous reports (WANG *et al.* 2013; THOMAS *et al.* 2014).

Given the importance of insulin receptor in glucose homeostasis (KITAMURA *et al.* 2003), we tested whether *Tg(U6x:sgRNA(insra/b); LC); Tg(actb2:cas9; LR)* double carriers with severe pigmentation defects had defective glucose metabolism. At 6 dpf, the double carriers had similar fasting total free glucose content to single carrier siblings (Fig 3G). However, after feeding with 5% chicken egg yolk (MADDISON and CHEN 2012) (CARTEN *et al.* 2011), the glucose levels increased almost 2-fold in double carriers, but remained unchanged in single carrier siblings (n=5, $P<0.01$) (Fig 3G). Thus, transgenic expression of *cas9* and sgRNA targeting *insra* and *insrb* resulted in impairment of glucose homeostasis.

Conditional CRISPR/Cas9 mutagenesis in transgenic fish

The primary impetus for the above experiments was to develop CRISPR/Cas9-based conditional mutagenesis. This can be achieved through regulated expression/availability of either *cas9* or *sgRNA*. To temporally control *cas9* expression, we generated *Tg(hsp70:loxP-mCherry-STOP-loxP-cas9)* lines (referred as *Tg(HotCre:cas9))*, to allow heat-shock induction of *cas9* expression in a Cre-dependent manner (Hesselson et al, 2009). As a proof of principle experiment, we injected *in vitro* transcribed Cre mRNA into zygotes from *Tg(HotCre:cas9) x Tg(U6a:tyr(sgRNA); LC)* to remove the "STOP", and heat-shocked the progeny at 6 or 24 hours postfertilization (hpf) to induce *cas9.* All *Tg(HotCre:cas9); Tg(U6a:tyr(sgRNA); LC)* double carriers had hypopigmentation phenotypes (Fig 4A). In the absence of either Cre mRNA or heat-shock, no pigmentation phenotypes were detectable

(Fig 4A). The degree of mutagenesis in these embryos, as determined by HMA (Fig 4B), was slightly lower than in larvae with constitutive expression of *cas9*.

To spatially control Cas9 expression, we generated *Tg(fabp10:cas9, CG)* lines in which *cas9* expression is liver-specific. These fish were crossed to *Tg(U6x:sgRNA(insra/b); LC)* to obtain double carriers. To determine whether liver-specific mutagenesis occurred in the double carriers, we assessed mutagenesis at *insra* and *insrb* loci in liver and muscle at one month of age. HMA indicated that close to 60% of the *insra* and *insrb* loci were mutated in the liver (Fig 5A). Considering that hepatocytes constitute about 75% of the liver at this stage (NI *et al.* 2012), the fraction of mutant alleles in *cas9*-positive cells is close to 80%, similar to that in the ubiquitous *cas9* lines. We did not detect mutations in skeletal muscle, confirming tissue-specificity of mutagenesis (Fig 5A).

Insulin signaling in liver promotes glycogen synthesis and suppresses gluconeogenesis. Loss of *insra*/*b* function in the liver impairs glucose homeostasis. In mice with liver-specific disruption of insulin receptor (LIRKO), fasting blood glucose levels are lower and fed blood glucose levels are higher at 6 months of age due to impaired glycogen storage and weakened suppression of gluconeogenesis, respectively (MICHAEL *et al.* 2000). To test whether the CRISPR/Cas9-mediated liver mutagenesis is sufficient to impair glucose metabolism, we determined fasting and postprandial blood glucose in three-month-old *Tg(fabp10:cas9, CG); Tg(U6x:sgRNA(insra/b); LC)* fish. Fasting and postprandial glucose levels were measured a week apart in the same group of fish. Compared to wild type controls, the *Tg(fabp10:cas9, CG); Tg(U6x:sgRNA(insra/b); LC)* fish had lower fasting glucose levels (27.36±4.15 vs 37.53±2.24 mg/dl, $p<0.037$), but markedly higher postprandial glucose (190.97±29.70 vs 59.01±11.50 mg/dl, $p<0.001$) (Fig 5B). Thus, the phenotypes in the Cre-

mediated, conditional LIRKO mouse were recapitulated using liver-specific inactivation of insulin receptor genes in zebrafish using CRISPR/Cas9.

The tissue-specificity of mutagenesis may also be achieved by targeted delivery of sgRNAs. To test this possibility, we targeted *ascl1a* that is essential for Müller glia dedifferentiation and retina regeneration in zebrafish (RAMACHANDRAN *et al.* 2010). Two sgRNAs targeting *ascl1a* were synthesized *in vitro* (Fig 6A) and delivered into one eye of dark-adapted *Tg(actb2:cas9: LR)* adults by injection followed by electroporation. After 48-hour exposure to constant, high intensity light to induce photoreceptor degeneration and Müller glia proliferation, the number of proliferating cells in both eyes was assessed using PCNA immunofluorescence. The number of PCNA+ progenitor cells in the inner nuclear layer of the sgRNA(*ascl1a*)-exposed retina was decreased by 5-fold, to a mean of less than 9 compared to an average of more than 45 in the sgRNA(*EGFP*)-injected control retinas ($P<0.01$) (Fig 6B, 6C). The data indicate that spatial and temporal specific mutagenesis can be achieved by controlling either *cas9* expression or sgRNA delivery.

DISCUSSION

Spatially and temporally controlled gene inactivation is critical for understanding detailed gene function. We show here that the recently developed CRISPR mutagenesis can be adopted for controlled mutagenesis in zebrafish.

Our data indicate that transgenically expressed *cas9* and sgRNA can cause biallelic gene inactivation in somatic cells in a controllable fashion. Although CRISPR mutagenesis using stable transgenic lines expressing both *cas9* and sgRNA have been used for generating both germline and somatic mutations in non-vertebrate models such as *C. elegans* and *D.*

melanogaster (PORT *et al.* 2014; SHEN *et al.* 2014; XUE *et al.* 2014), it has not been reported in vertebrates until our manuscript was being revised (ABLAIN *et al.* 2015). A Cas9 knock-in mouse line has been used to achieve tissue-specific mutagenesis (PLATT *et al.* 2014; SWIECH *et al.* 2015). However, in those reports, sgRNA was delivered by virus or nanoparticles rather than a transgenic approach. Although viral and nanoparticle delivery of sgRNA has many advantages, not every tissue/organ is accessible by this approach. Even in accessible tissues/organs, not all cells are equally targeted. For zebrafish, a reliable method of virus- or nanoparticle-mediated gene expression is not available. However, we achieved retinal specific inactivation of *ascl1a* using targeted injection of sgRNA followed by electroporation. Other methods, such as lipofection (ANDO and OKAMOTO 2006) (CHANG *et al.* 2014), may also be used for targeted delivery of sgRNA, though specificity and accessibility remain a concern. Transgenic lines with spatial and temporal control of *cas9* expression are a better choice for achieving desired control of mutagenesis in somatic cells. Although it requires the availability of suitable *cas9* lines, the high efficiency of transgenesis and the availability of many characterized tissue-specific promoters in zebrafish make this a straightforward and efficient process. The collection of Gal4 enhancer trap lines may also be used to direct UAS driven tissue-specific expression of *cas9* (SCOTT *et al.* 2007; KAWAKAMI *et al.* 2010). Several inducible expression systems, such at heat shock (HALLORAN *et al.* 2000), tetracycline (KNOPF *et al.* 2010), and RU468 (EMELYANOV and PARINOV 2008) have been successfully adapted into zebrafish and could be used to achieve spatial and temporal control of *cas9* expression. Our *Tg(HotCre:cas9)* lines should provide both spatial and temporal control (HESSELSON *et al.* 2009).

Conditional CRISPR mutagenesis may be a viable alternative to Cre/Flp-dependent conventional approaches. The observed indel frequency caused by cas9 is comparable to

the recombination frequency induced by Cre/Flp. A major advantage of conditional CRISPR mutagenesis is that it does not require a pre-engineered conditional allele. Although a large collection of conditional alleles is available in mice (SKARNES *et al.*), in general a conditional allele is time consuming to generate. Another advantage of conditional CRISPR mutagenesis is that only two elements, *cas9* and sgRNA, need to be bred together for conditional CRISPR mutagenesis, compared to three (two mutant alleles and a Cre/Flp transgene) for the conventional approach. This will decrease at least one generation of breeding. Finally, conditional CRISPR mutagenesis can target multiple genes simultaneously, while conventional conditional mutagenesis requires extensive breeding to achieve multiplex mutagenesis. Although conditional CRISPR mutagenesis does require the generation of sgRNA-expressing lines, this is much easier than generating an engineered conditional allele. The disadvantage of conditional CRISPR mutagenesis is that the mutations are very heterogeneous, while precise mutations are generated with the conventional approach. This can lead to a significant decrease of bialllelic inactivation if the targeted region is tolerant of in-frame deletions. In such a scenario, only about 2/3 indels maybe loss-of-function, resulting in biallelic inactivation in only 4/9 cases. An advantage of our system is that it allows for targeting multiple sites in a single gene. If two distant sites are chosen, independent mutagenesis at each site would decrease the frequency of potentially hypomorphic small in-frame indels from 1/3 to 1/9. The deletion of the intervening sequence should further lower the frequency of hypomorphic alleles. If only one sgRNA is used for a gene, it is critical to target functionally important regions of a gene for conditional CRISPR mutagenesis so that even in-frame deletions result in severe loss of function.

We found that the phenotype severity induced by CRISPR/Cas9-mediated somatic mutagenesis is not uniform among siblings. The major cause may be individual difference in

mutation rates. This could be due to different levels of cas9 or sgRNA expression since some of our transgenic fish carry more than 1 transgene insertion. Nevertheless, similar variation has been observed in flies when each of the transgenes is a single insertion at a defined genomic locus (PORT *et al.* 2014). Another cause may be the heterogeneity of the mutations. The mutated fish are highly mosaic at the target sites with some indels impairing function more than others. Individual animals likely have a different complement of mutations from each other, leading to phenotypic variation.

There is a high degree of correlation among the indel frequencies at different targets within the same fish. This suggests that the level of mutagenesis of one target can serve as an indicator for the rest. For ubiquitous mutagenesis, *tyr* is a good indicator target because of its restricted expression in pigmented cells and its easily visible phenotype due to biallelic inactivation. This allows easy identification of mutant fish. In addition, hypopigmentation minimizes the interference of fluorescence detection, facilitating fluorescent marker-based genetic or chemical screens for modifiers of mutant phenotype. For tissue-specific gene inactivation, however, other easily scorable markers need to be developed.

Taken together, our findings demonstrate transgenic expression of cas9 and sgRNA is sufficient to generate extensive biallelic somatic mutations for functional analysis. The mutagenesis may be multiplexed for increased efficiency, eliminating redundancy, and/or analysing gene-gene interaction. Multiplex conditional mutagenesis can be achieved by inducible or tissue-specific expression of cas9, or by tissue-specific delivery of sgRNAs.

ACKNOWLEDGEMENTS

We thank Amanda Goodrich and Corey Guthrie of VUMC zebrafish facility for expert care of zebrafish, Baishali Maskeri, Alice Young and Robert Blakesley of NIH Intramural Sequencing

Center (NISC) for providing sequencing data. This work was supported by the Vanderbilt Diabetes Research and Training Centre, the National Institutes of Health [DK088686 to WC, R01 EY024354 to JGP, and intramural research grants to SMB] and the American Diabetes Association [1-13-BS-027 to WC].

REFERENCES

ABLAIN, J., E. M. DURAND, S. YANG, Y. ZHOU and L. I. ZON, 2015 A CRISPR/Cas9 Vector System for Tissue-Specific Gene Disruption in Zebrafish. Dev Cell 32: 756-764.

ANDO, H., and H. OKAMOTO, 2006 Efficient transfection strategy for the spatiotemporal control of gene expression in zebrafish. Mar Biotechnol (NY) 8: 295-303.

BIESECKER, L. G., and N. B. SPINNER, 2013 A genomic view of mosaicism and human disease. Nat Rev Genet 14: 307-320.

BOONANUNTANASARN, S., S. PANYIM and G. YOSHIZAKI, 2008 Characterization and organization of the U6 snRNA gene in zebrafish and usage of their promoters to express short hairpin RNA. Mar Genomics 1: 115-121.

CARTEN, J. D., M. K. BRADFORD and S. A. FARBER, 2011 Visualizing digestive organ morphology and function using differential fatty acid metabolism in live zebrafish. Dev Biol 360: 276-285.

CERMAK, T., E. L. DOYLE, M. CHRISTIAN, L. WANG, Y. ZHANG *et al.*, 2011 Efficient design and assembly of custom TALEN and other TAL effector-based constructs for DNA targeting. Nucleic Acids Res 39: e82.

CHANG, N., C. SUN, L. GAO, D. ZHU, X. XU *et al.*, 2013 Genome editing with RNA-guided Cas9 nuclease in zebrafish embryos. Cell Res 23: 465-472.

CHANG, T. Y., P. SHI, J. D. STEINMEYER, I. CHATNUNTAWECH, P. TILLBERG *et al.*, 2014 Organ-targeted high-throughput in vivo biologics screen identifies materials for RNA delivery. Integr Biol (Camb) 6: 926-934.

CHEN, B., L. A. GILBERT, B. A. CIMINI, J. SCHNITZBAUER, W. ZHANG *et al.*, 2013 Dynamic imaging of genomic loci in living human cells by an optimized CRISPR/Cas system. Cell 155: 1479-1491.

CLARKE, B. D., D. M. CUMMINS, K. A. MCCOLL, A. C. WARD and T. J. DORAN, 2012 Characterization of Zebrafish Polymerase III Promoters for the Expression of Short-Hairpin RNA Interference Molecules. Zebrafish.

DIETZL, G., D. CHEN, F. SCHNORRER, K. C. SU, Y. BARINOVA *et al.*, 2007 A genome-wide transgenic RNAi library for conditional gene inactivation in Drosophila. Nature 448: 151-156.

DOUDNA, J. A., and E. CHARPENTIER, 2014 Genome editing. The new frontier of genome engineering with CRISPR-Cas9. Science 346: 1258096.

EMELYANOV, A., and S. PARINOV, 2008 Mifepristone-inducible LexPR system to drive and control gene expression in transgenic zebrafish. Dev Biol 320: 113-121.

GAGNON, J. A., E. VALEN, S. B. THYME, P. HUANG, L. AHKMETOVA *et al.*, 2014 Efficient mutagenesis by Cas9 protein-mediated oligonucleotide insertion and large-scale assessment of single-guide RNAs. PLoS One 9: e98186.

GU, H., J. D. MARTH, P. C. ORBAN, H. MOSSMANN and K. RAJEWSKY, 1994 Deletion of a DNA polymerase beta gene segment in T cells using cell type-specific gene targeting. Science 265: 103-106.

HALBIG, K. M., A. C. LEKVEN and G. R. KUNKEL, 2008 Zebrafish U6 small nuclear RNA gene promoters contain a SPH element in an unusual location. Gene 421: 89-94.

HALLORAN, M. C., M. SATO-MAEDA, J. T. WARREN, F. SU, Z. LELE *et al.*, 2000 Laser-induced gene expression in specific cells of transgenic zebrafish. Development 127: 1953-1960.

HESSELSON, D., R. M. ANDERSON, M. BEINAT and D. Y. STAINIER, 2009 Distinct populations of quiescent and proliferative pancreatic {beta}-cells identified by HOTcre mediated labeling. Proc Natl Acad Sci U S A.

HIGASHIJIMA, S., H. OKAMOTO, N. UENO, Y. HOTTA and G. EGUCHI, 1997 High-frequency generation of transgenic zebrafish which reliably express GFP in whole muscles or the whole body by using promoters of zebrafish origin. Dev Biol 192: 289-299.

HSU, P. D., E. S. LANDER and F. ZHANG, 2014 Development and applications of CRISPR-Cas9 for genome engineering. Cell 157: 1262-1278.

HWANG, W. Y., Y. FU, D. REYON, M. L. MAEDER, S. Q. TSAI *et al.*, 2013 Efficient genome editing in zebrafish using a CRISPR-Cas system. Nat Biotechnol 31: 227-229.

JAO, L. E., S. R. WENTE and W. CHEN, 2013 Efficient multiplex biallelic zebrafish genome editing using a CRISPR nuclease system. Proc Natl Acad Sci U S A 110: 13904-13909.

KANE, D. A., and C. B. KIMMEL, 1993 The zebrafish midblastula transition. Development 119: 447-456.

KAWAKAMI, K., G. ABE, T. ASADA, K. ASAKAWA, R. FUKUDA *et al.*, 2010 zTrap: zebrafish gene trap and enhancer trap database. BMC Dev Biol 10: 105.

KITAMURA, T., C. R. KAHN and D. ACCILI, 2003 Insulin receptor knockout mice. Annu Rev Physiol 65: 313-332.

KNOPF, F., K. SCHNABEL, C. HAASE, K. PFEIFER, K. ANASTASSIADIS *et al.*, 2010 Dually inducible TetON systems for tissue-specific conditional gene expression in zebrafish. Proc Natl Acad Sci U S A 107: 19933-19938.

KRAUSS, J., P. ASTRINIDIS, H. G. FROHNHOFER, B. WALDERICH and C. NUSSLEIN-VOLHARD, 2013 transparent, a gene affecting stripe formation in Zebrafish, encodes the mitochondrial protein Mpv17 that is required for iridophore survival. Biol Open 2: 703-710.

KWAN, K. M., E. FUJIMOTO, C. GRABHER, B. D. MANGUM, M. E. HARDY *et al.*, 2007 The Tol2kit: a multisite gateway-based construction kit for Tol2 transposon transgenesis constructs. Dev Dyn 236: 3088-3099.

LI, M., L. A. MADDISON, P. PAGE-MCCAW and W. CHEN, 2014 Overnutrition induces beta-cell differentiation through prolonged activation of beta cells in zebrafish larvae. Am J Physiol Endocrinol Metab.

MADDISON, L. A., and W. CHEN, 2012 Nutrient excess stimulates beta-cell neogenesis in zebrafish. Diabetes 61: 2517-2524.

MICHAEL, M. D., R. N. KULKARNI, C. POSTIC, S. F. PREVIS, G. I. SHULMAN *et al.*, 2000 Loss of insulin signaling in hepatocytes leads to severe insulin resistance and progressive hepatic dysfunction. Mol Cell 6: 87-97.

MOSIMANN, C., C. K. KAUFMAN, P. LI, E. K. PUGACH, O. J. TAMPLIN *et al.*, 2011 Ubiquitous transgene expression and Cre-based recombination driven by the ubiquitin promoter in zebrafish. Development 138: 169-177.

NI, J. Q., M. MARKSTEIN, R. BINARI, B. PFEIFFER, L. P. LIU *et al.*, 2008 Vector and parameters for targeted transgenic RNA interference in Drosophila melanogaster. Nat Methods 5: 49-51.

NI, T. T., J. LU, M. ZHU, L. A. MADDISON, K. L. BOYD *et al.*, 2012 Conditional control of gene function by an invertible gene trap in zebrafish. Proc Natl Acad Sci U S A 109: 15389-15394.

OTA, S., Y. HISANO, M. MURAKI, K. HOSHIJIMA, T. J. DAHLEM *et al.*, 2013 Efficient identification of TALEN-mediated genome modifications using heteroduplex mobility assays. Genes Cells 18: 450-458.

PARICHY, D. M., D. G. RANSOM, B. PAW, L. I. ZON and S. L. JOHNSON, 2000 An orthologue of the kit-related gene fms is required for development of neural crest-derived xanthophores and a subpopulation of adult melanocytes in the zebrafish, Danio rerio. Development 127: 3031-3044.

PLATT, R. J., S. CHEN, Y. ZHOU, M. J. YIM, L. SWIECH *et al.*, 2014 CRISPR-Cas9 knockin mice for genome editing and cancer modeling. Cell 159: 440-455.

PORT, F., H. M. CHEN, T. LEE and S. L. BULLOCK, 2014 Optimized CRISPR/Cas tools for efficient germline and somatic genome engineering in Drosophila. Proc Natl Acad Sci U S A 111: E2967-2976.

RAJARAM, K., E. R. SUMMERBELL and J. G. PATTON, 2014 Technical brief: Constant intense light exposure to lesion and initiate regeneration in normally pigmented zebrafish. Mol Vis 20: 1075-1084.

RAMACHANDRAN, R., B. V. FAUSETT and D. GOLDMAN, 2010 Ascl1a regulates Muller glia dedifferentiation and retinal regeneration through a Lin-28-dependent, let-7 microRNA signalling pathway. Nat Cell Biol 12: 1101-1107.

SCHNUTGEN, F., S. DE-ZOLT, P. VAN SLOUN, M. HOLLATZ, T. FLOSS *et al.*, 2005 Genomewide production of multipurpose alleles for the functional analysis of the mouse genome. Proc Natl Acad Sci U S A 102: 7221-7226.

SCOTT, E. K., L. MASON, A. B. ARRENBERG, L. ZIV, N. J. GOSSE *et al.*, 2007 Targeting neural circuitry in zebrafish using GAL4 enhancer trapping. Nat Methods 4: 323-326.

SEARLE, A. G., 1990 Comparative genetics of albinism. Ophthalmic Paediatr Genet 11: 159-164.

SHEN, Z., X. ZHANG, Y. CHAI, Z. ZHU, P. YI *et al.*, 2014 Conditional knockouts generated by engineered CRISPR-Cas9 endonuclease reveal the roles of coronin in C. elegans neural development. Dev Cell 30: 625-636.

SKARNES, W. C., B. ROSEN, A. P. WEST, M. KOUTSOURAKIS, W. BUSHELL *et al.*, A conditional knockout resource for the genome-wide study of mouse gene function. Nature 474: 337-342.

SUNG, Y. H., J. M. KIM, H. T. KIM, J. LEE, J. JEON *et al.*, 2014 Highly efficient gene knockout in mice and zebrafish with RNA-guided endonucleases. Genome Res 24: 125-131.

SWIECH, L., M. HEIDENREICH, A. BANERJEE, N. HABIB, Y. LI *et al.*, 2015 In vivo interrogation of gene function in the mammalian brain using CRISPR-Cas9. Nat Biotechnol 33: 102-106.

TEER, J. K., L. L. BONNYCASTLE, P. S. CHINES, N. F. HANSEN, N. AOYAMA *et al.*, 2010 Systematic comparison of three genomic enrichment methods for massively parallel DNA sequencing. Genome Res 20: 1420-1431.

THOMAS, H. R., S. M. PERCIVAL, B. K. YODER and J. M. PARANT, 2014 High-throughput genome editing and phenotyping facilitated by high resolution melting curve analysis. PLoS One 9: e114632.

THUMMEL, R., S. C. KASSEN, J. E. MONTGOMERY, J. M. ENRIGHT and D. R. HYDE, 2008 Inhibition of Muller glial cell division blocks regeneration of the light-damaged zebrafish retina. Dev Neurobiol 68: 392-408.

TOYOSHIMA, Y., C. MONSON, C. DUAN, Y. WU, C. GAO *et al.*, 2008 The role of insulin receptor signaling in zebrafish embryogenesis. Endocrinology.

URASAKI, A., G. MORVAN and K. KAWAKAMI, 2006 Functional dissection of the Tol2 transposable element identified the minimal cis-sequence and a highly repetitive sequence in the subterminal region essential for transposition. Genetics 174: 639-649.

WANG, H., H. YANG, C. S. SHIVALILA, M. M. DAWLATY, A. W. CHENG *et al.*, 2013 One-step generation of mice carrying mutations in multiple genes by CRISPR/Cas-mediated genome engineering. Cell 153: 910-918.

XUE, Z., M. WU, K. WEN, M. REN, L. LONG *et al.*, 2014 CRISPR/Cas9 mediates efficient conditional mutagenesis in Drosophila. G3 (Bethesda) 4: 2167-2173.

YU, C., Y. ZHANG, S. YAO and Y. WEI, 2014 A PCR based protocol for detecting indel mutations induced by TALENs and CRISPR/Cas9 in zebrafish. PLoS One 9: e98282.

ZANG, L., Y. SHIMADA, Y. NISHIMURA, T. TANAKA and N. NISHIMURA, 2013 A novel, reliable method for repeated blood collection from aquarium fish. Zebrafish 10: 425-432.

FIGURE LEGENDS

Figure 1. Efficient disruption of *tyr* by transgenic Cas9 and sgRNA(tyr). A. Experimental schematic of transgenic CRISPR mutagenesis. Transgenic lines with various *cas9* expression patterns were generated, including *Tg(ubi:cas9; CG)* and *Tg(actb2:cas9; LR)* with ubiquitous expression, *Tg(HotCre:cas9; CG)* with heat shock inducible expression, and *Tg(fabp10:cas9; CG)* with liver specific expression. *Tg(U6: sgRNA(goi); LC*) line were generated to

ubiquitously express sgRNAs targeting the gene of interest. The fluorescent markers allowed non-invasive genotyping of the progeny. CG, *cmlc2:EGFP*, green heart; LR, *cryaa:tagRFP*, red lens; LC, *cryaa:mCerulean*. B-G. Images of three-day-old embryos indicating biallelic mutations evidenced by loss of pigmentation in the retinal pigment epithelium. Representative images from three transgenic genotypes are shown from *Tg(ubi:cas9)* x *Tg(U6a:sgRNA(tyr))* (B-D) and *Tg(actb2:cas9)* x*Tg (U6a:sgRNA(tyr))* (E-G). H. HMA showing efficient *tyr* mutagenesis in *cas9*/sgRNA double transgenic larvae at 5 dpf. Controls were sibling *Tg (U6a:sgRNA(tyr))* larvae at the same age. Both *Tg(ubi:cas9; CG)* and *Tg(actb2:cas9; LR)* were able to induce efficient mutagenesis. The numbers below each lane are the fraction of heteroduplex quantified by densitometry. I. Comparison of HMA and qPCR-based assessment of mutagenesis efficiency. The same PCR products in H. were analysed by qPCR using two sets of primers, one amplifying both wild type and mutant alleles while the other only amplifying the wild type allele.

Figure 2. Development of a system for multiplex CRISPR/Cas9 mutagenesis. A. Pairwise sequence comparison of the identity of the five zebrafish U6 promoters. B. Semi-quantitative RT-PCR analysis showing lower U6e promoter activity in embryos at 24 hpf injected with *Tg(U6a:sgRNA(atp2a2a); U6b:sgRNA(atp2a2b); U6c:sgRNA(nf1a); U6b:sgRNA(nf1b); U6c:sgRNA(dmd); LC)*. Controls were non-injected siblings at the same stage. C. Semi-quantitative RT-PCR analysis showing lower U6e promoter activity in F1 *Tg(U6a:sgRNA(tyr); U6b:sgRNA(fms); U6c:sgRNA(mpv17); LC)* larvae at 5 dpf. Controls were non-transgenic siblings at the same stage. D. Schematic showing Golden Gate assembly of transgenic lines, including five sgRNAs-expressing cassettes using four distinct zebrafish U6 promoters. Colour triangles indicate BsaI distinct overhangs.

Figure 3. Simultaneous inactivation of *insra and insrb* impairs glucose homeostasis. A. Schematic of the sgRNA-expressing transgene. B. Sequence of *insra* and *insrb* target regions. C. RT-PCR analysis indicating that four distinct U6 promoters (U6a, U6b, U6c, U6d) have similar activity in directing *sgRNA(insra)* and *sgRNA(insrb)* expression in F1 transgenic larvae at 5 dpf. Controls were non-transgenic larvae at the same stage. D. HMA showing efficient mutagenesis at *tyr*, *insra* and *insrb* loci in double transgenic larvae (samples 1-6) at 6 dpf. Arrows indicate smaller *insra* and *insrb* products that are from alleles with deletion between the 2 targets. E. Positive correlation among the *tyr*, *insra* and *insrb* mutation rate (*tyr* vs *insra*, r2=0.72; *tyr* vs *insrb*, r2=0.71). Mutation rate was calculated from sequencing data of 17 *Tg(actb2:cas9; (U6x:sgRNA(insra/b)* fish from two founders. F. *Tg(actb2:cas9; (U6x:sgRNA(insra/b)* individuals share a set of highly prevalent alleles. The frequency of the top 2 *tyr* alleles and top 3 *insra* and *insrb* alleles in 5 siblings are shown. Del indicates the allele resulting from deletion of the sequence between the 2 DBSs in *insra* and *insrb*. #1 and #2 indicate the number 1 and 2 most frequent alleles other than the deletion. G. Fasting and postprandial glucose levels (mean±SE) in six-day-old double transgenic larvae before and after incubation in 5% egg yolk solution for 2h. A significant increase was observed in double positive larvae (n=5, t test, $P<0.01$) after feeding.

Figure 4. Temporal-specific CRISPR/Cas9 mutagenesis. A. Heat shock-inducible *tyr* inactivation. Cre RNA was injected into 1-cell stage embryos from *Tg(HotCre:cas9)* x *Tg(U6a:sgRNA(tyr); LC)*. Uninjected embryos were used as controls. The embryos were heat shocked at 6 or 24 hpf. Pigmentation phenotypes were induced in Cre RNA-injected double carriers (top) but not uninjected double carriers (bottom). Images were taken at 5 dpf. B. HMA results of *tyr* locus in Cre RNA-injected, heat shocked *Tg(HotCre:cas9)*;*Tg(U6a:sgRNA(tyr); LC)* double carriers (mean±SE, n=4).

Figure 5. Liver-specific CRISPR/Cas9 mutagenesis of *insra* and *insrb* impairs glucose homeostasis. A. HMA results indicating liver-specific mutagenesis. Liver and muscle from one month-old *Tg(fabp10:cas9; CG); (U6x:sgRNA(insra/b); LC)* fish were analysed. B. Impaired glucose metabolism in *Tg(fabp10:cas9; CG); (U6x:sgRNA(insra/b); LC)* fish. Fasting and postprandial glucose levels (mean±SE) were measured in 3 month-old transgenic fish and wild type control fish. Transgenic fish (n=8) had lower fasting glucose and higher postprandial glucose than wild type control fish (n=10); t test, * $P<0.05$, **$p<0.01$.

Figure 6. Retinal-specific CRISPR/Cas9 mutagenesis of *ascl1a* by targeted delivery of sgRNA suppresses damage-induced regeneration. A. Sequence of *ascl1a* target regions. B. Fewer proliferative cells were detected in *Tg(actb2:cas9; LR)* retinas after *sgRNA(ascl1a)* injection than *sgRNA(EGFP)*-injected retinas. Scale bar, 60 μm. C. Quantification of (B). A significant decrease of PCNA+ cell was observed (mean±SE, non-parametric Mann-Whitney U test, $P<0.01$).

Fig 1

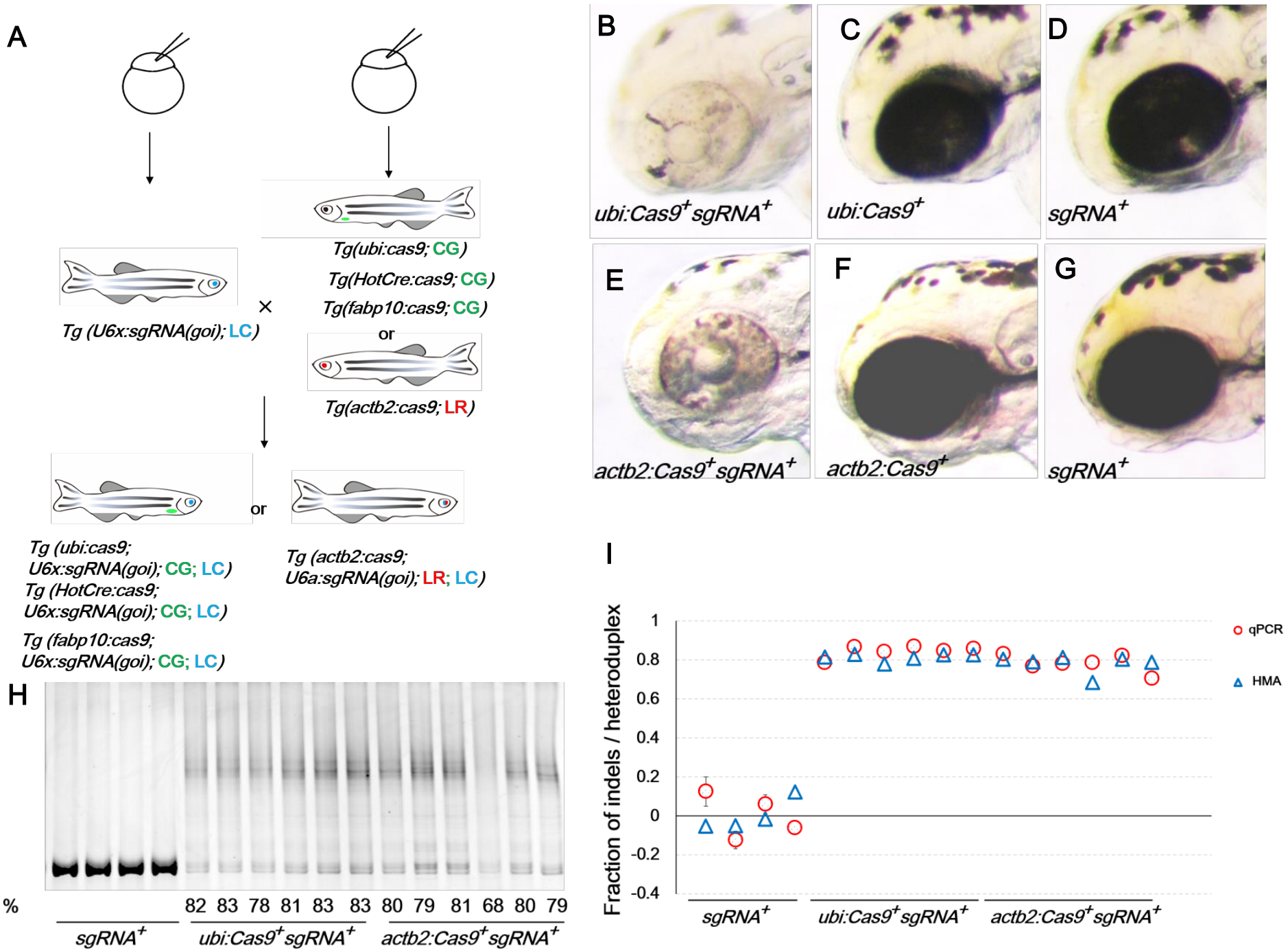
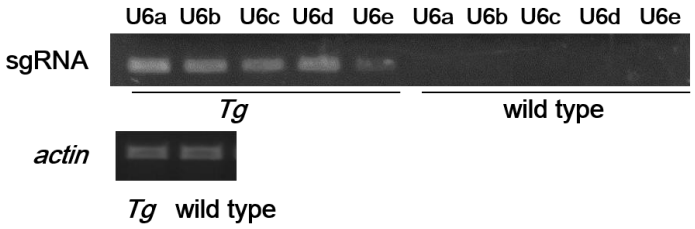

A
Tg(ubi:cas9; CG)
Tg(HotCre:cas9; CG)
Tg(fabp10:cas9; CG)
or
Tg(actb2:cas9; LR)
Tg (U6x:sgRNA(goi); LC)
×
or
Tg (ubi:cas9; U6x:sgRNA(goi); CG; LC)
Tg (HotCre:cas9; U6x:sgRNA(goi); CG; LC)
Tg (fabp10:cas9; U6x:sgRNA(goi); CG; LC)
Tg (actb2:cas9; U6a:sgRNA(goi); LR; LC)
B
ubi:Cas9+ sgRNA+
C
ubi:Cas9+
D
sgRNA+
E
actb2:Cas9+ sgRNA+
F
actb2:Cas9+
G
sgRNA+
H
%
82 83 78 81 83 83 80 79 81 68 80 79
sgRNA+
ubi:Cas9+ sgRNA+
actb2:Cas9+ sgRNA+
I
Fraction of indels / heteroduplex
1
0.8
0.6
0.4
0.2
0
-0.2
-0.4
qPCR
HMA
sgRNA+
ubi:Cas9+ sgRNA+
actb2:Cas9+ sgRNA+

Fig 2

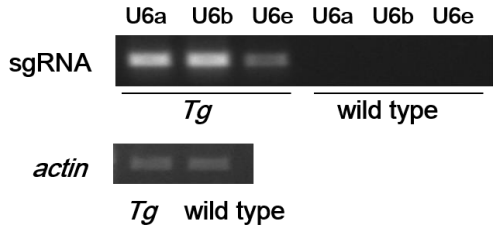
A

	U6a	U6b	U6c	U6d	U6e
U6a		61.36	63.01	65.99	36.84
U6b	61.36		67.18	56.62	36.91
U6c	63.01	67.18		60.61	38.95
U6d	65.99	56.62	60.61		37.86
U6e	36.84	36.91	38.95	37.86	

B



C



D

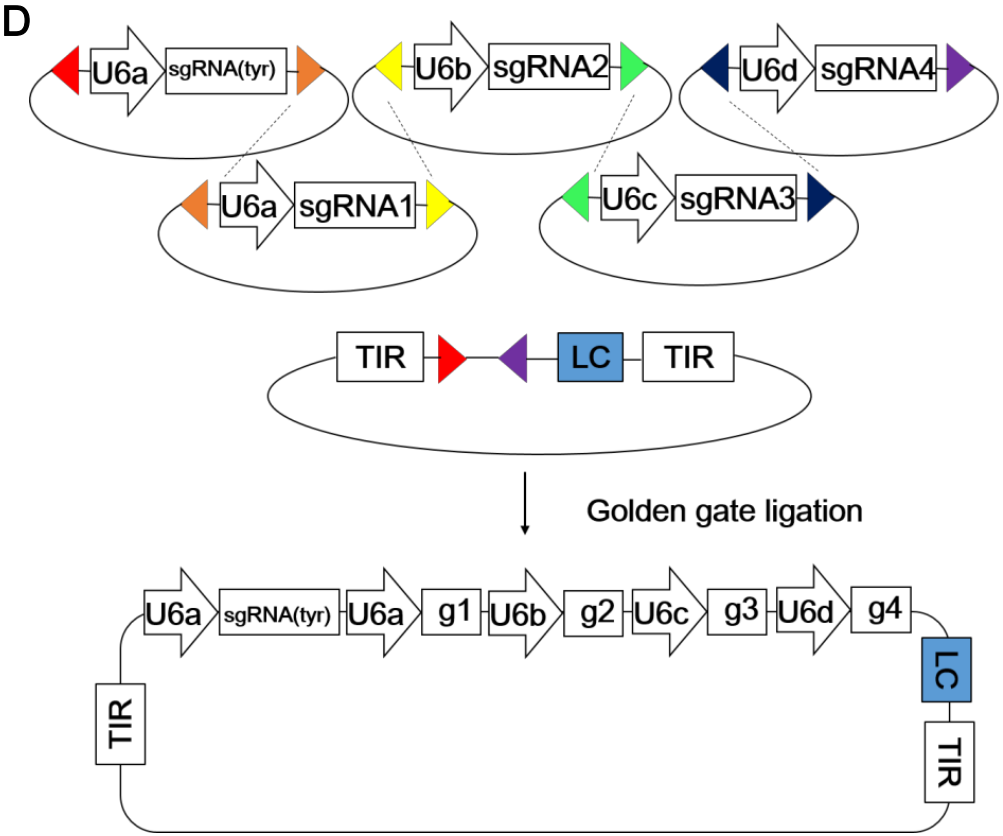


Fig 3

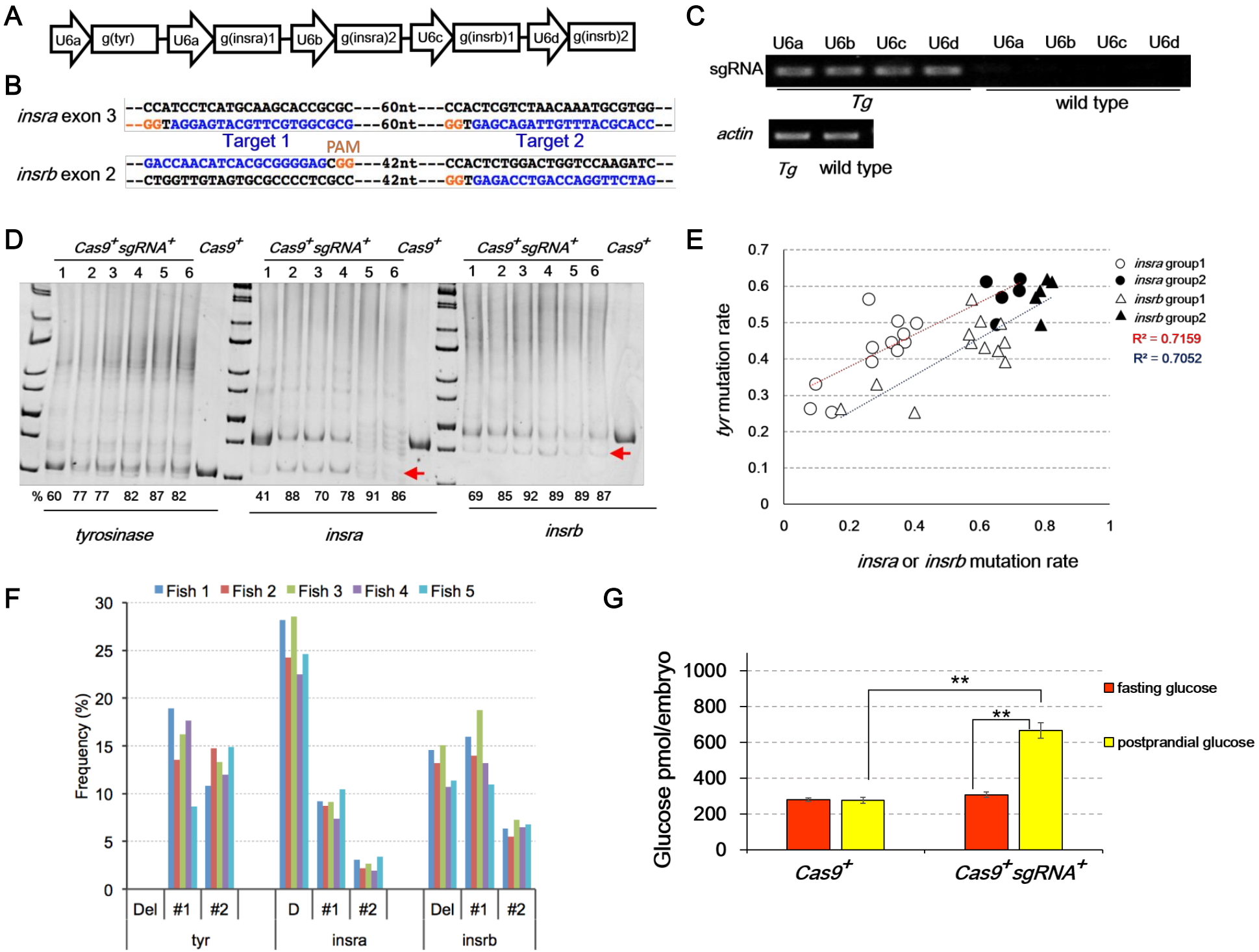
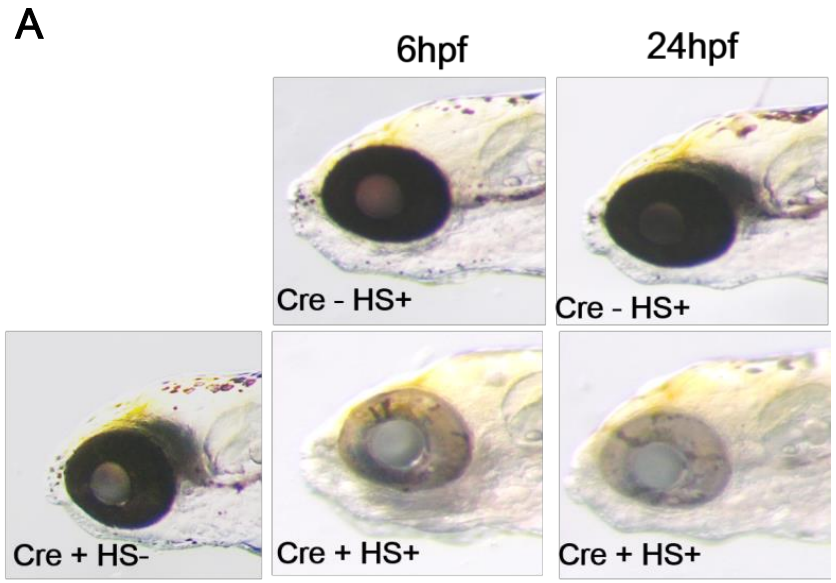

A
U6a
g(tyr)
U6a
g(insra)1
U6b
g(insra)2
U6c
g(insrb)1
U6d
g(insrb)2
B
insra exon 3
--CCATCCTCATGCAAGCACCGCGC---60nt---CCACTCGTCTAACAAATGCGTGG--
--GGTAGGAGTACGTTCGTGGCGCG---60nt---GGTGAGCAGATTGTTTACGCACC--
Target 1
PAM
Target 2
insrb exon 2
--GACCAACATCACGCGGGGAGCGG---42nt---CCACTCTGGACTGGTCCAAGATC--
--CTGGTTGTAGTGCGCCCCTCGCC---42nt---GGTGAGACCTGACCAGGTTCTAG--
C
U6a U6b U6c U6d U6a U6b U6c U6d
sgRNA
Tg
wild type
actin
Tg wild type
D
Cas9+sgRNA+ Cas9+ Cas9+sgRNA+ Cas9+ Cas9+sgRNA+ Cas9+
1 2 3 4 5 6 1 2 3 4 5 6 1 2 3 4 5 6
% 60 77 77 82 87 82 41 88 70 78 91 86 69 85 92 89 89 87
tyrosinase
insra
insrb
E
tyr mutation rate
insra or insrb mutation rate
insra group1
insra group2
insrb group1
insrb group2
R² = 0.7159
R² = 0.7052
F
Fish 1 Fish 2 Fish 3 Fish 4 Fish 5
Frequency (%)
Del #1 #2 D #1 #2 Del #1 #2
tyr
insra
insrb
G
Glucose pmol/embryo
fasting glucose
postprandial glucose
**
**
Cas9+
Cas9+sgRNA+

Fig 4


A
6hpf
24hpf
Cre - HS+
Cre - HS+
Cre + HS-
Cre + HS+
Cre + HS+

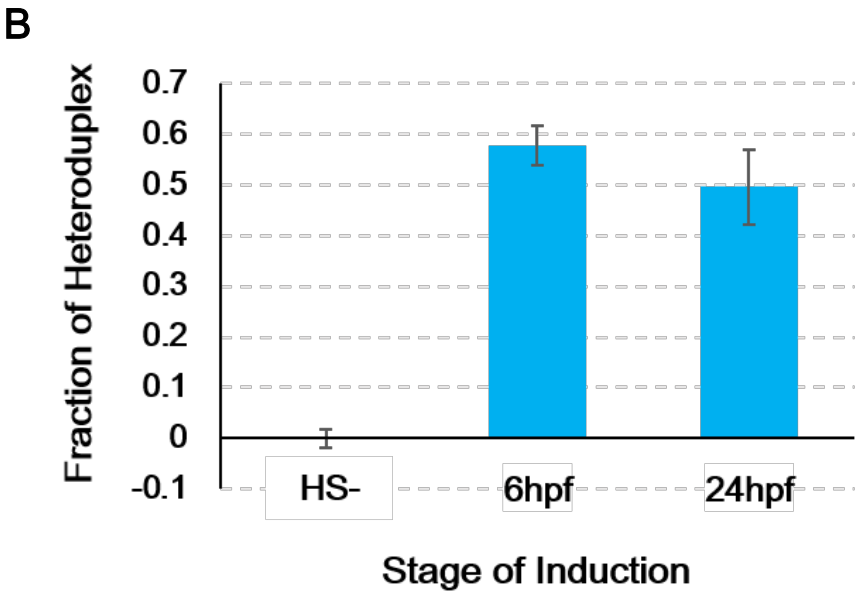

B
Fraction of Heteroduplex
0.7
0.6
0.5
0.4
0.3
0.2
0.1
0
-0.1
HS-
6hpf
24hpf
Stage of Induction

Fig 5

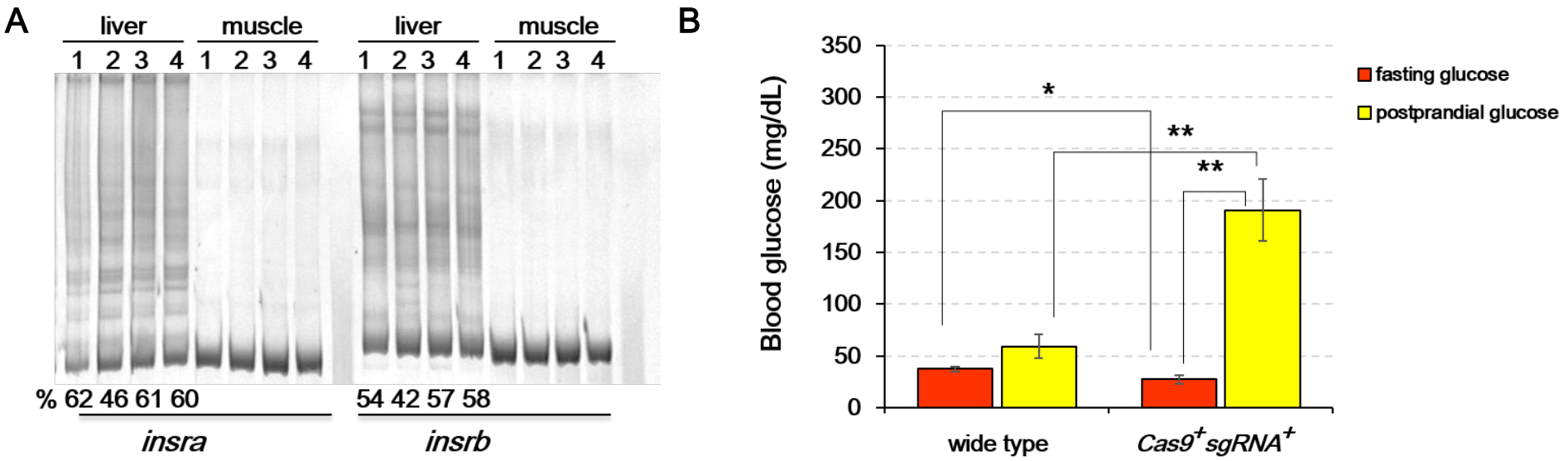
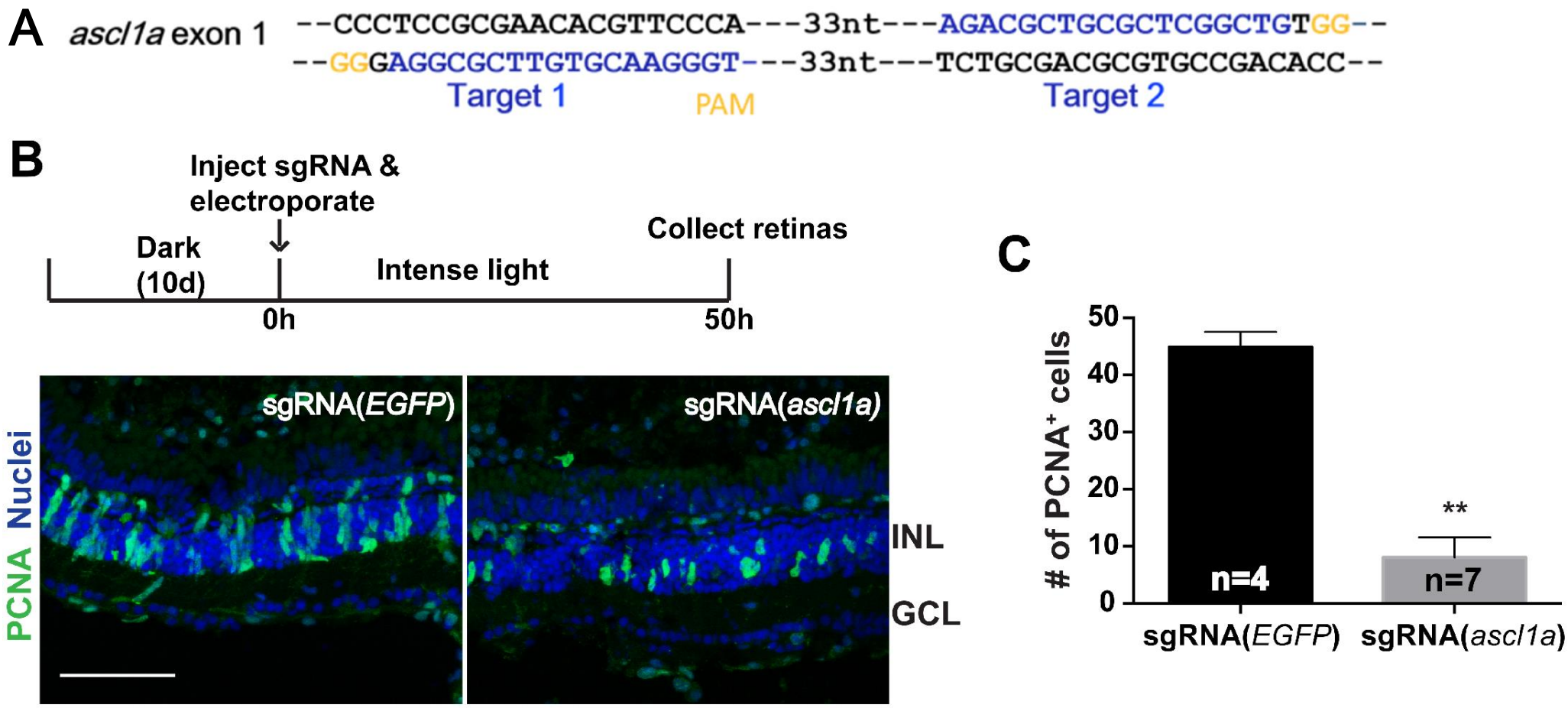

A
liver
muscle
liver
muscle
1 2 3 4 1 2 3 4 1 2 3 4 1 2 3 4
% 62 46 61 60
54 42 57 58
insra
insrb
B
Blood glucose (mg/dL)
350
300
250
200
150
100
50
0
*
**
**
fasting glucose
postprandial glucose
wide type
Cas9+sgRNA+

Fig 6


A
ascl1a exon 1
--CCCTCCGCGAACACGTTCCCA---33nt---AGACGCTGCGCTCGGCTGTGG--
--GGGAGGCGCTTGTGCAAGGGT---33nt---TCTGCGACGCGTGCCGACACC--
Target 1
PAM
Target 2
B
Inject sgRNA &
electroporate
Dark
(10d)
Intense light
Collect retinas
0h
50h
sgRNA(EGFP)
sgRNA(ascl1a)
PCNA Nuclei
INL
GCL
C
# of PCNA+ cells
50
40
30
20
10
0
n=4
n=7
**
sgRNA(EGFP)
sgRNA(ascl1a)